IEEE Transactions on Nuclear Science, Vol. NS-24, No. 3, June 1977

# BEAM MODULATOR FOR AN ELECTRON LINAC

G. Rouse, R. Siemann, and M. Tigner
Laboratory of Nuclear Studies, Cornell University
Ithaca, N. Y. 14853


## Summary

A system has been developed for modulating the beam of the Cornell Electron Storage Ring injection linac. It employs a sub-modulated, high frequency Lissajous raster of the electron beam on a collimator, followed by a subharmonic prebunching. In conjunction with a two amp electron gun, a variable pattern of single, one nanocoulomb, S-band bunches is produced. The Lissajous raster is generated by two orthogonal pairs of deflection plates attached to high frequency resonant coaxial lines. Submodulation of the raster is accomplished by a single pair of upstream of deflection plates driven by a broad band miniature tetrode. Details of the design calculations, hardware, and performance are given.


## Introduction

The proposed techniques for coalescing beam bunches in the Cornell Storage Ring (CESR) require the electron linac to produce intense, single S-band bunches spaced at 42 nS. Typical intensities required are 4 x $10^{-10}$ coulombs per bunch, and the number of such bunches must remain variable at this time due to the different requirements of several proposed coalescing schemes. A beam modulator has been designed, constructed and tested to meet these requirements. The modulator consists of a chopper to produce the 42nS structure (the r.f. chopper of Figure 1), a subharmonic prebuncher to give the necessary intensity, and a second chopper (the pulsed chopper) which works in conjunction with the r.f. chopper to control the number of bunches.

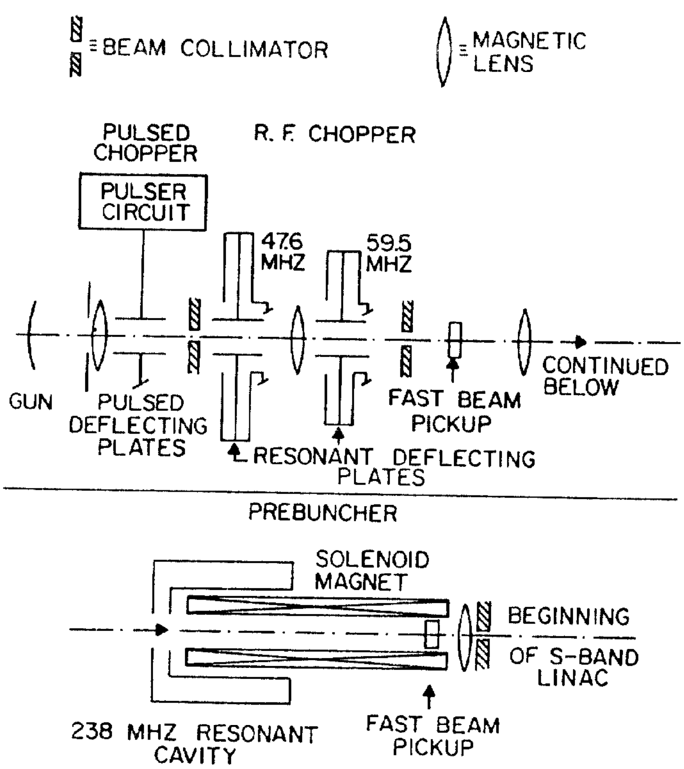


Figure 1: Schematic of the beam modulator

## Gun and Pulsed Chopper

The linac gun we are using is a Varian MkIV gun; the gun has been run at typically 110kV and 1A for the modulator tests. The gun anode focuses the beam about 10cm from the anode; the exact location of the focal spot is controlled by a magnetic lens just after the anode. A collimator with a 3mm dia hole is located at the focal position and this collimator defines the size of the beam. A set of deflecting plates between the anode and the collimator controls the length of the beam pulse. These plates are 8cm long and shaped like sections of a 2cm dia cylinder; they are driven by a fast pulse circuit which uses an Eimac Y540 tetrode as the switching element. To minimize stray capacitance, the circuit is mounted as close as is feasible to the chopping plates. By applying a 10nS rise time, 3kV amplitude pulse to the plates, the pulsed chopper can move the beam away from the collimating hole between the beam bursts from the r.f. chopper.

## RF Chopper

We chose a prebunching frequency of 238 MHz (the 12th subharmonic of the linac frequency of 2856 MHz) because it gave a sufficient increase in intensity without excessively high prebunching power and voltage. Once this choice was made, the length of the beam burst from the r.f. chopper which could be bunched and accepted by the linac in a single S-band bunch was found to be 1.4nS (at the base). This was selected as the design value for the chopper.

This time of 1.4nS, the beam spot size, and the size of the hole in the chopper collimator determine the rate at which the beam must be swept across the chopping hole. The peak deflecting voltage is

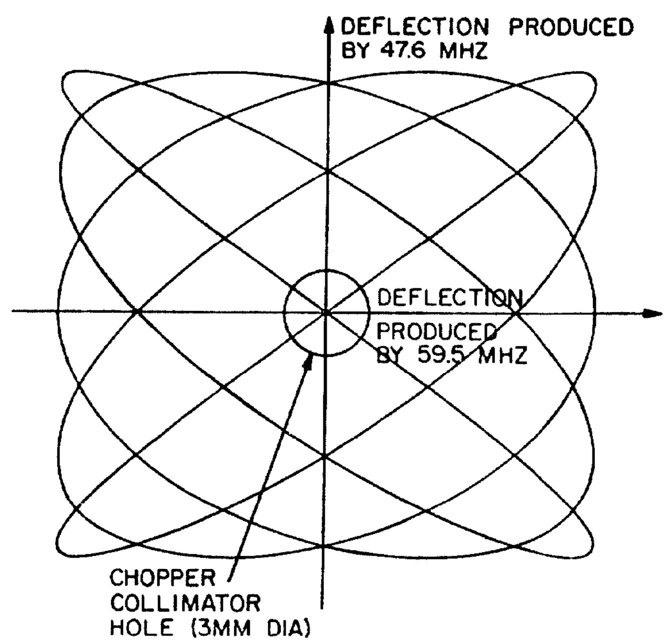


Figure 2: The beam path produced by the application of different r.f. frequencies to orthogonal deflecting plates.

---

Work supported by the National Science Foundation.

determined by this rate; were the r.f. frequency a variable, this voltage would be inversely proportional to the frequency for fixed deflecting plate separation. In practice, the plate separation also needs to be increased as the frequency decreases to accommodate the increased amplitude of the beam motion. Both effects increase the needed r.f. power. The frequency, of course, is not a variable; the desired 42nS beam burst spacing determines the frequency. We found that with the 11.9 MHz r.f. frequency that is necessary for our application, the r.f. voltage and power requirements were excessive.

These problems are not nearly so severe if two frequencies are used to produce the chopping. By using different frequencies to produce orthogonal deflections, a Lissajous Pattern (such as the one in Figure 2) is obtained. This particular pattern is drawn for our choice of frequencies of 47.6 MHz on the y axis and 59.5 MHz on the x axis. These are the 4th and 5th harmonics of 11.9 MHz. The beam crosses the chopping hole at the required frequency and at the desired rate. Going to higher frequencies reduces the r.f. power, but also reduces the distance between the chopping hole and points of closest approach by the beam.

At the beam currents necessary to give the desired intensity, the beam optics is dominated by space charge forces. To keep the maximum beam size small, we decided to make the distance between the collimating holes of the pulsed chopper and the r.f. chopper 40cm. Therefore, we had to place the deflecting plates on different sides of a magnetic lens and then rotate the 47.6 MHz plates to compensate for the $40^{\circ}$ rotation imparted by the lens.

Resonant quarter wave lines driven with opposite phases are attached to the deflecting plates. The coupling from the r.f. power source to the resonant lines is designed to accommodate the rather heavy beam loading of the 2A beam.

The chopper performance is shown in Figure 3. The beam is being detected with a capacitive pickup as described by Koontz and Miller[1]. The desired 42nS separation is achieved, and the beam has the desired width with deflecting voltage of approximately 5kV across each pair of plates.

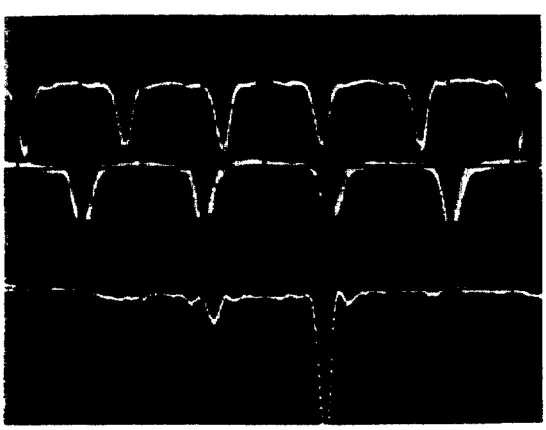

Figure 3: R.F. chopper performance. The top two traces are the chopped beam when only one pair of deflecting plates was deiven. The bottom trace is for both pairs driven. Time scale: 5 ns/cm.

Prebuncher

The prebuncher compresses the beam in length by applying a velocity modulation. With beams of our intensity, this bunching action is affected significantly by space charge forces. In the drift space between the prebunching cavity and the accelerator entrance, these forces tend to cause the beam to debunch and to blow up radially. The debunching must be understood when choosing the prebuncher voltage and the drift space length.

A computer program was written to understand debunching effects. For simplicity, only longitudinal motion was studied, and the beam was assumed to be confined to a 5mm radius by a set of solenoid magnets. The beam was split into small pancakes; at position $z_i$ the pancake has a mean velocity $v_i$ and a thickness $w_i$. At time $t + \Delta t$, $z_i$ and $v_i$ are given by

$$v_i(t + \Delta t) = v_i(t) + \frac{e}{m} E_z(z_i(t), t)\Delta t$$

$$z_i(t + \Delta t) = z_i(t) + v_i(t)\Delta t + \frac{1}{2}\frac{e}{m} E_z(z_i(t), t)\,(\Delta t)^2$$

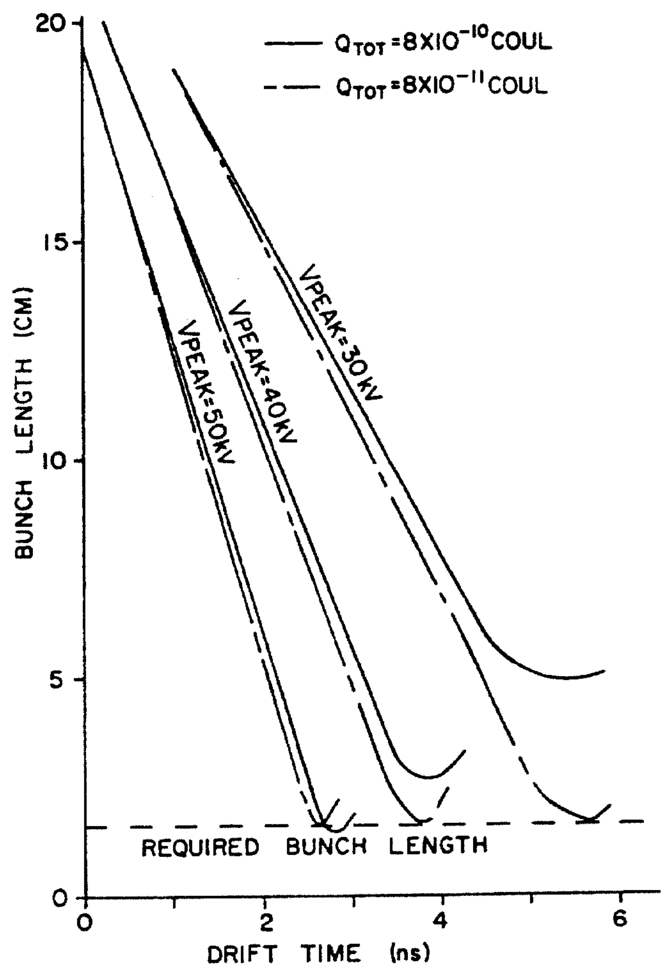


Figure 4: Results of a calculation of bunch length versus drift time. Lengths and times are measured in the frame of reference discussed in the text, and zero time corresponds to the time when the last electron leaves the bunching cavity.

and the width by

$$w_i(t + \Delta t) = \frac{z_{i+1}(t + \Delta t) - z_{i-1}(t + \Delta t)}{2}$$

The electric field ($E_z$) was calculated using a numerical solution of Laplace's equation. For simplicity in treating relativistic effects the program worked in an initial frame of reference with a velocity equal to that of a 110kV electron. The results are presented as the bunch length vs the drift time (both measured in this inertial frame), and are presented in Figure 4 for charges of $8 \times 10^{-11}$ coul, and $8 \times 10^{-10}$ coul in the bunch. Short drift times and large peak bunching voltages are necessary to compensate for space charge debunching.

We chose a drift time of 2.8nS which corresponds to 65cm in the laboratory and a prebunching voltage of 50kV. The prebunching cavity is essentially a resonant quarter wave line with a capacitive gap at one end (see Figure 5). The beam travels through this gap and the "center conductor" of the resonant line. The cavity does not seem to exhibit any beam loading at the beam currents ($\sim 4 \times 10^{-10}$ coul/bunch) that we have run to date.

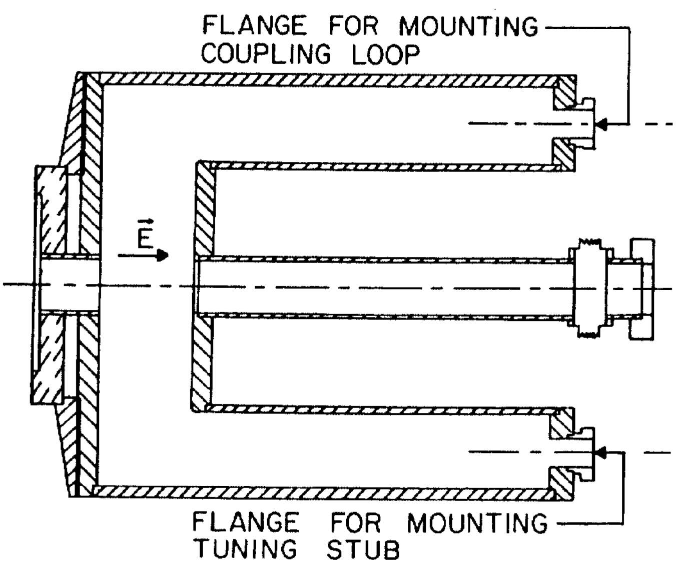


Figure 5: Diagram showing the construction of the prebunching cavity.

The beam is contained radially by a system of solenoids which provide an achromatic optical system for the beam. Numerous miscellaneous beam components including a second capacitive beam detector are contained in the drift space. The prebuncher has been tested and its performance is shown in Figure 6. There is a clear enhancement in the instantaneous current and a clear decrease in the width of the beam pulse. We believe the observed width is due to the frequency response of the beam detector. We plan tests in the near future with the chopper and prebuncher combined with the linac buncher section. These tests will give us the first solid confirmation that we have achieved the desired bunching.

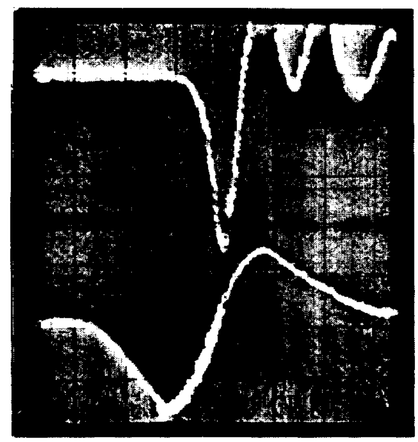

Figure 6: Prebuncher performance. The bottom trace (20 mV/cm) is the beam with zero prebuncher voltage. The top trace (50 mV/cm) is the beam with the prebuncher cavity turned on.
Time scale: 0.5 ns/cm.


References

1. R. F. Koontz and R. H. Miller, Proc. IEEE NS22, No. 3, 1350, (1975).